Dalton Transactions

Accepted Manuscript

ROYAL SOCIETY OF CHEMISTRY

www.rsc.org/dalton

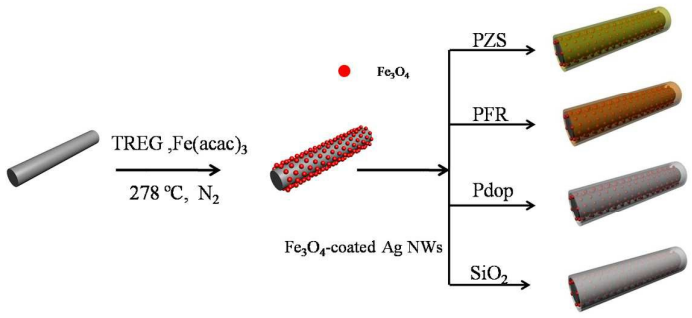

The Ag NWs/Fe_3O_4 composites were synthesized by high-temperature decomposition, which can be coated by various polymers to widen the application.

Journal Name

RSCPublishing

ARTICLE

Large-Scale Fabrication and Application of Magnetite Coated Ag NWs-Core Water-Dispersible Hybrid Nanomaterials

Cite this: DOI: 10.1039/x0xx00000x

Received 00th January 201x,
Accepted 00th January 201x

DOI: 10.1039/x0xx00000x

www.rsc.org/

Baoyu Wang, Min Zhang,* Weizhen Li, Linlin Wang, Jing Zheng, Wenjun Gan,* Jingli Xu*

In this work, we report a large scale synthetic procedure that allows attachment of magnetite nanoparticles onto the Ag NWs in situ, which was conducted in triethylene glycol (TREG) solution with iron acetylacetonate and Ag NWs as starting materials. The as-prepared Ag NWs/Fe_3O_4 NPs composites are well characterized by SEM, TEM, XRD, XPS, FT-IR, and VSM techniques. It was found that the mass ratio of iron acetylacetonate to Ag NWs plays crucial role in controlling the amount of magnetite nanoparticles decorated on the Ag NWs. The resultant Ag NWs/Fe_3O_4 NPs composites exhibit super-paramagnetic properties at room temperature, and can be well dispersed in aqueous and organic solutions, which is greatly beneficial for the application and functionality. Thus, the as-prepared magnetic silver nanowire show good catalytic activity, using the catalytic reduction of methylene blue (MB) as a model reaction. Furthurmore, the Ag NWs/Fe_3O_4 NPs composites can be functionalized by the polydopamine(Pdop), resorcinol–formaldehyde resin(PFR), and SiO_2, respectively, in aqueous/ethanol solution. Meanwhile it can also be coated by polyphosphazene(PZS) in organic solution, resulting in the unique nanocable with well-defined core shell structures. Besides, take Ag NWs/Fe_3O_4@SiO_2 for example, the hollow magnetic silica nanotube can be obtained with the use of Ag NWs as physical template by use of a solution made of ammonium and H_2O_2. These can widely improve the application of the Ag NWs/Fe_3O_4 NPs composites. As-synthesized above nanocomposites have high potential for applications in the fields of polymer, wastewater treatment, sensors, and biomaterials.

Introduction

Nowadays, the synthesis of multi-component hybrid nanostructures by combining two or more different components into a single object has attracted considerable attention [1-11]. Such multi-component nanoparticles NPs can not only combine different functionalities of the individual constituents but also show unique and superior properties different form the individual component, therefore, providing potential applications in many fields.[9] Up to now, various hybrid nanomaterials have been successfully synthesized by using different template cores such as graphene,[2] carbon nanotubes,[3] carbon fiber[4],noble metal,etc.[5-8] Among them, the hybrid nanomaterials based on one-dimensional (1D) nanostructure cores are of particular interest due to their improved or novel properties and thus promising applications in the fields of optics, electronics, and optoelectronics.[9-11] Recently, one dimensional materials especially silver nanowires (Ag NWs) have attracted considerable interest due to their intriguing electrical, thermal, and optical properties. Notably, as a noble metal with high electrical conductivity and good resistance to corrosion,[9-10] Ag nanowires (NWs) have been applied in a wide variety of devices such as robust flexible electronics and mesh transparent electrodes.[13] Additionally, Ag NWs tend to establish perfect networks rather than common silver particles because slender fillers with high aspect ratios are capable of easily forming a continuous network at a lower loading level than sphere fillers. Moreover, the Ag NWs coated with noble metal, metal oxide nanoparticles, i.e., the formation of Ag NWs-based hybrid nanomaterials, can combine the features of each component, which may result in novel chemical and physical properties, and thus greatly widening their applications. As a result, more and more attention has been paid on Ag NWs-based hybrid nanomaterials, and several types of Ag NWs-based hybrid nanomaterials such as Ag NWs/ZnO(NPs),[11] Ag NWs/ZnO(nanopyramids), [12] Ag NWs/ZnO(Nanorods), [13] Ag NWs/Nickel shell,[14] Ag NWs/Cu_2O,[15] Ag NWs/ TiO_2,[16,17] Ag NWs/ Ag-Pd, [18] Ag NWs/AgCl, [19, 20] Ag NWs/Ag_3PO4, [21, 22] and Ag NWs/Fe_3O_4[23] have been prepared by various methods including spray coating process, sonochemistry, and hydrothermal procedure. Among these Ag NWs hybrids, the Magnetic Ag NWs/Fe_3O_4 NPs nanocomposites with both electrical and magnetic properties are receiving great attentions due to their potential applications such as catalytic reduction agents,[18] photothermal probes[19] and in biomedicine.[20,21] Recently, magnetic CNTs composites have been emerging to advanced research owing to their potential applications in microwave adsorption, electrochemical biosensor et al. [5] Meanwhile, the Magnetic Ag NWs/Fe_3O_4 NPs nanocomposites have significant advantages over other magnetic CNTs hybrids because of the robust interaction between noble metals and magnetic CNTs groups for bioapplication. Additionally, magnetic-nanoparticle coated Ag NWs might be controlled to align in three dimensions as carbon nanotubes (CNTs) to increase the mechanical and electrical properties of polymers with an external magneticfield, [23-25] Moreover, the successful research on Fe_3O_4-coated CNTs has provided evidence for decoration of one dimensional (1D) nanostructure materials with nano-sized magnetic Fe_3O_4.[26] Although various methods have been developed for the preparation of Fe_3O_4 on the surfaces of Ag NWs, including co-precipitation method, [23] hydrothermal method, [24] these systems still suffer from drawbacks such as low yield of the product, and ferromagnetic property. Thus, the exploration of simple and efficient methods for the large-scale synthesis of 1-D coaxial hetero-structures is still a great challenge.

In this paper, we describe a simple approach of decoration of Ag NWs with magnetite nanoparticles by in situ high-temperature decomposition of the precursor iron(III) acetylacetonate and Ag NWs in liquid polyols. The size of magnetite nanoparticles and their coverage density on the surface of Ag NWs are both tunable in this method, which offers an efficient way for fine tailoring the magnetic properties of the final nanocomposites. It is worth mentioning that triethylene glycol (TREG) was selected as solvent and a reducing agent in this synthesis, which endows the assembled nanostructures stabilizing with a layer of hydrophilic polyol molecules and thus good water-dispersibility. Thus, the as-prepared magnetic silver nanowire show good catalytic activity, using the catalytic reduction of MB as a model reaction. More importantly, the SiO_2, PFR, Pdop, were selected to coat the Ag NWs/Fe_3O_4 NPs composites in aqueous/ethanol solution, while the PZS was selected to coat the Ag NWs/Fe_3O_4 NPs composites in organic solution. These coating process can widely improve the application of the resulting composites. Besides, the magnetic hollow silica nanotube can be obtained by removing the silver core by use of a solution made of ammonia and H_2O_2. The water dispersible and superparamagnetic nanocomposites at room temperature have significant potential for application in the fields of composites, wastewater treatment, sensors, and biomaterials.

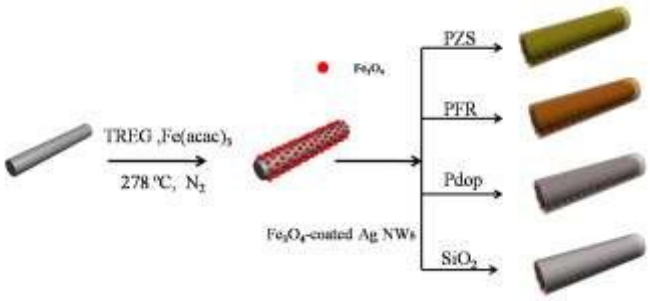

Scheme 1 Synthesis route of Ag NWs/Fe_3O_4 NPs composites and functionalization by PZS, PFR, Pdop, SiO_2.

Scheme 1 shows the process flow to fabricate the nano-hybrides and the structure of the AgNWs. First, high-quality AgNWs with length of 4–15 um were synthesized by a previously reported facile and scalable one-pot synthesis(Supporting Information).[27] Next, decoration of Ag NWs with magnetite nanoparticles by in situ high-temperature decomposition of the precursor iron(III) acetylacetonate and Ag NWs in liquid were obtained. Finally, the SiO_2, PFR, Pdop, PZS were selected to coat the Ag NWs/Fe_3O_4 NPs composites to improve the functionality of the resultant composites.

Experimental Section

Materials

$AgNO_3$ was purchased from Shanghai Reagent Factory. PVP (Mn=40000)was purchased from Yonghua Chemical Technology co., Ltd. (Jiangsu.China). Iron(III) acetylacetonate ($Fe(acac)_3$, 99%) was from energy chemical. Triethylene glycol (TREG, 99%) and glycerol were purchased from SCRC. Formaldehyde solution, Phosphonitrilic

chloride trimer(HCCP) and 4,4'-Diaminodiphenyl ether(DDE) were purchased from aladdin. Resorcine and triethylamine were purchased from shanghai Lingfeng chemical reagent co., Ltd. Dopamine hydrochloride was purchased from Alfa Aesar co., Ltd (shanghai China). All other reagents used were analytical grade.

Preparation of Ag NWs/Fe_3O_4 NPs composites.

Ag NWs were synthesized *via* a typical method similar to that reported previously. 10 mL Ag NWs(10 mg/mL) ethanol solution and 30 mL triethylene glycol add to the flask, and the mixture was then heated to 95°C to remove ethanol. After the ethanol was removed completely, 150 mg of the iron precursor $Fe(acac)_3$ and 30 mL triethylene glycol were added to the flask. The solution was sonicated for 5 min. Finally, the resulting mixture was then heated to 278 °C under vigorous stirring and N_2 protection and kept at reflux for 30 min. After cooling to room temperature, 60 mL ethanol was added to dilute the solution. Then the obtained composites were magnetically separated by a commercial magnet ,which was washed with ethanol several times. The obtained was centrifuged at 4000 rpm for several times until the centrifugal supernatant fluid was colorless transparent and dried in vacuum. The obtained product was about 130 mg. We also increase the amount of silver nanowires(200 mg) and $Fe(acac)_3$(300 mg) with fixing the volume of triethylene glycol to 60 mL, 270 mg of the product can be easily obtained, which keeps with the similar morphology as before.

Catalytic Properties of the Ag NWs/Fe_3O_4 NPs **composites**

The reduction of MB by $NaBH_4$ was chosen as a model reaction for the efficiency testing of the Ag NWs/Fe_3O_4 NPs composite. A given amount of the magnetic catalysts were added into the mixture of $NaBH_4$ and MB (40 mg/L) .The colour of the mixture gradually vanished, indicating the reduction of the MB dye. Changes in the concentration of MB were monitored by examining the variations in the maximal UV-Vis absorption at 665 nm. After the catalytic reaction was completed, the nanocatalysts were separated by externally applied magnetic field and then repeated for the catalytic reaction. The recyclability of the nanoparticle catalysis was determined by measuring the maximal UV-Vis absorption of MB at the end of each catalytic degradation reaction.

Functionalization of Ag NWs/Fe_3O_4 NPs composites by PZS, PFR, Pdop, SiO_2.

The experimental details are shown in the surporting information.

Characterization

The morphology of the Ag NWs/Fe_3O_4 NPs composites was observed using a scanning electron microscope (SEM, Hitachi S-8000, Japan) in a secondary electron scattering mode at 5 kV and a transmission electron microscope (TEM). X-Ray powder diffraction (XRD) patterns of the products were recorded with a Rigaku D/max-γB diffractometer equipped with a rotating anode and a Cu Kα source (l = 0.154 nm). The energy-dispersive X-ray spectrometer (EDS) data were obtained on a JEOL JEM 2010 electron microscope at an accelerating voltage of 200 kV. X-Ray photoemission spectroscopy (XPS) data wre obtained with an ESCALAB 250Xi instrument equipped with a monochromatic Al anode X-ray gun. Fourier transform infrared spectroscopy (FT-IR) spectra were obtained using a Perkin-Elmer Spectrum One spectrometer. And the magneticcharacterization of the Ag NWs/Fe_3O_4 NPs composites were carried out using a vibrating specimen magnetometer.

Results and discussion.

Fig. 1 shows the XRD patterns of the pristine Fe_3O_4 NPs, Ag NWs and the Ag NWs/Fe_3O_4 nanocomposites. The XRD pattern (Fig. 1a) of the Ag NWs shows broad diffraction peaks at 2θ= 38.2°, 44.5°, 64.4°, 77.5° respectively corresponding to the (111), (200), (220), and (311) reflection of silver, which match well with the data from the (JCPDS file No. 89-3722) for silver. From the XRD pattern of the Ag NWs/Fe_3O_4 hybrids, it is found that there are two new significant diffraction peaks at 2θ = 30.2°, 57.3° could be attributed to the structure (220) and (511) planes of the Fe_3O_4, which match well with the blue line for the magnetite the(JCPDS file No. 19-0629). The XRD pattern (Fig. 1a) of the Fe_3O_4 (blue line) shows broad diffraction peaks at 2θ = 30.2°, 35.6°, 43.3°, 57.3° and 62.8°, attributing to the (220), (311), (400), (511) and (440) reflection of Fe_3O_4. Fig. S1 shows the XRD patterns of the different weight ratio of Ag NWs/Fe_3O_4 composites. With the enlarging the weight ratio of the iron(III) acetylacetonate and Ag NWs, the peak intensity of Fe_3O_4 diffraction peaks become more and more distinct, due to the increasing coverage of Fe_3O_4 NPs on Ag NWs surface .

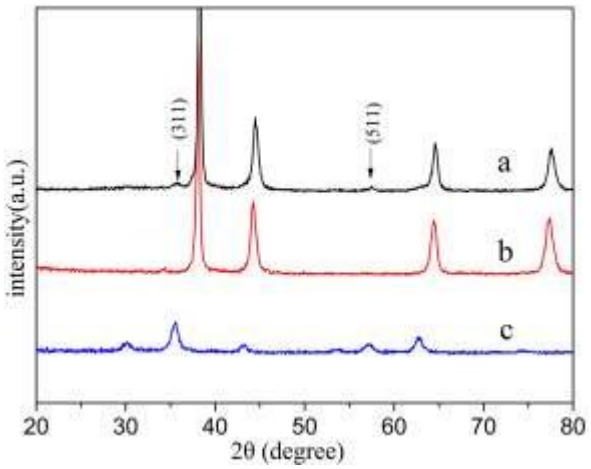

Fig. 1 X-Ray diffraction patterns of (a) Ag NWs/Fe_3O_4 NPs composites, (b) Ag NWs, and (c) standard XRD data for Fe_3O_4

In order to further clarify the phases of the as-prepared Ag NWs/Fe_3O_4 NPs composites, more evidence is provided by FT-IR. Fig. 2 shows FT-IR spectra of the pristine Fe_3O_4 NPs and the as-prepared Fe_3O_4-coated Ag NWs. For the Fe_3O_4, the characteristic band corresponding to the Fe–O bond was weakened and red-shifted to a higher wavenumber of 680 cm^{-1} compared to 630 cm^{-1} of the pristine Fe_3O_4,[28,29] which further confirms that the Fe_3O_4 nanoparticles are bound to the Ag NWs surface. Two characteristic bands at 2925–2809 cm^{-1} of C–H stretching and 1116–1050 cm^{-1} of C–O stretching in spectra confirm the attachment of TREG on the Fe_3O_4 and the Ag NWs/Fe_3O_4 surfaces. The broad band centered at 3411 cm^{-1} can be assigned to hydrogen bonded O–H stretching vibration arising from

hydroxyl groups on the surface of Fe_3O_4 and the adsorbed TREG and water on the surface of Fe_3O_4 decorated Ag NWs, which provide a strong evidence on good water dispersity of Ag NWs/Fe_3O_4 NPs composites. The absorption band at 1640 cm^{-1} on spectra refers to the vibration of remainder H_2O in the samples.[30]

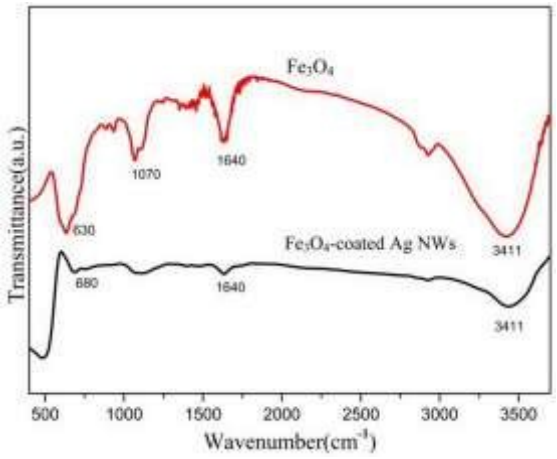

Fig. 2 FT-IR spectra of Fe_3O_4 nanoparticles and Ag NWs/Fe_3O_4 NPs composites

The morphologies of the samples were observed by SEM. Fig. 3(a,b) show SEM photographs of Ag nanowires, indicating that the surface of Ag nanowires with the length of 4-15 um are very smooth, and their diameter is about 100 nm. On the contrary, Ag NWs/Fe_3O_4 NPs composites display very rough surface morphologies, and a layer of tiny Fe_3O_4 nanoparticles is uniformly deposited on the surface of Ag nanowires. To get more information about the structure of Ag NWs/Fe_3O_4 NPs composites, it was further investigated by TEM.

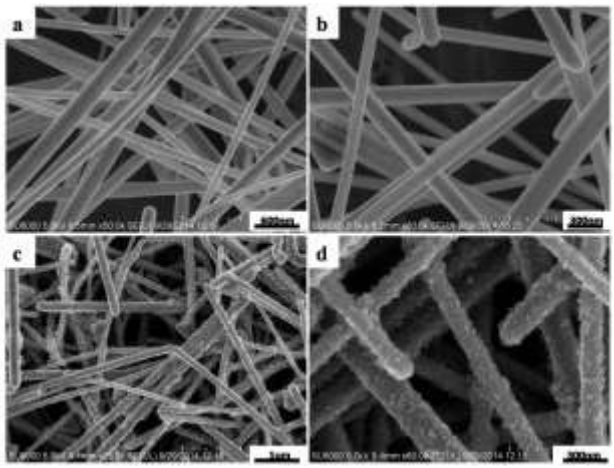

Fig. 3 SEM images of Ag NWs(a,b) and Ag NWs/Fe_3O_4 NPs composites (c,d)

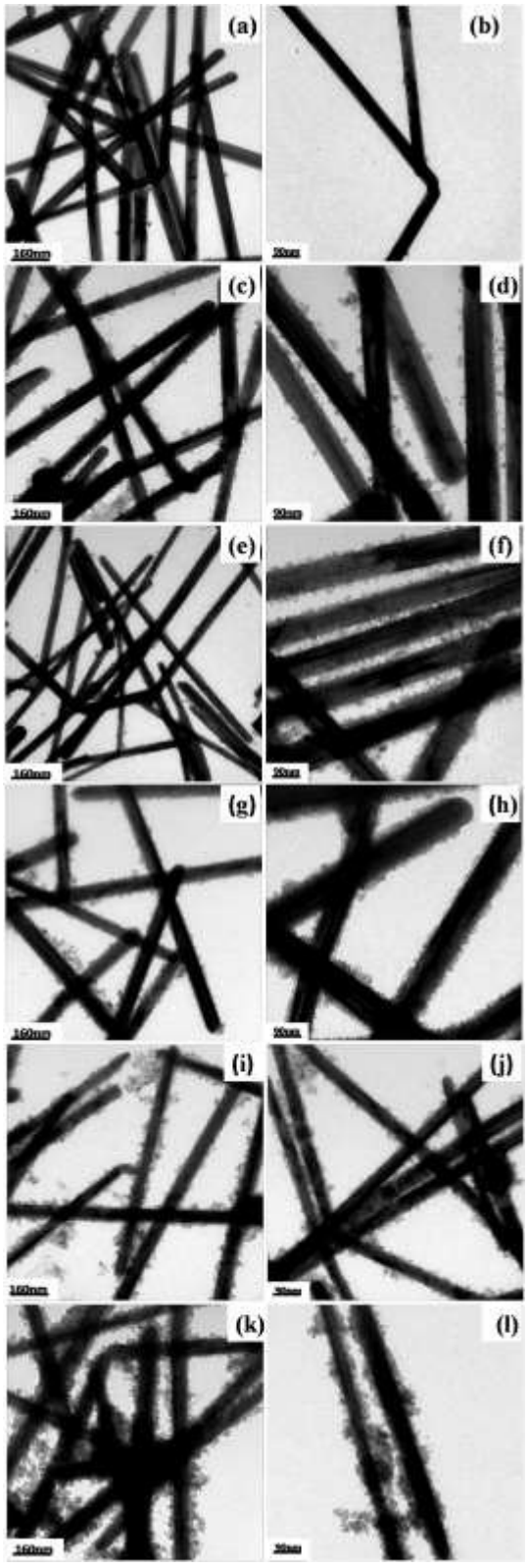

Fig. 4 TEM images of pure Ag NWs (a, b) and Ag NWs/Fe_3O_4 composites with increasing the weight ratio between $Fe(acac)_3$ and Ag NWs to 2 : 1(c,d), 1:1(e,f), 3:2(g,h), 1:2(i,j), 1:3(k,l).

The one-dimensional Ag NWs/Fe_3O_4 NPs composites were obtained when Ag nanowires were used as seeds. Compared to the

pure Ag nanowires shown in (Figure 4(a,b)), the size and the morphology of the Fe_3O_4 NPs decorated on Ag NWs were examined by TEM, of which the typical results are shown in Fig. 4(c-l). The effects of the concentration of the iron precursor and weight ratio to Ag NWs on the ultimate nanocomposite characteristics were investigated by performing a series of synthetic experiments at different reagents concentrations. It has been found that the coverage density can be easily controlled by changing the $Fe(acac)_3$ concentration and the weight ratio to Ag NWs. Fig. 4(c-l) show the different magnification TEM images of Ag NWs/Fe_3O_4 hybrids synthesized from different weight ratios of Ag nanowires to $Fe(acac)_3$. As shown in Fig. 4(c, d), when the $Fe(acac)_3$ weight ratio to Ag NWs was 2 : 1, the loading density of magnetite nanoparticles on Ag NWs was low, a lot of loose intermediate products of Fe_3O_4 nanoparticles were formed on the side walls of Ag NWs. It can also be seen that these shapeless intermediate products have gathered into relatively regular nanoparticles with sizes around 8 nm(Fig. S2). So it is sure that the formation of Fe_3O_4 nanoparticles was through an aggregation process of subparticles that is influenced strongly by the presence of TREG. When the $Fe(acac)_3$ weight ratio to Ag NWs was increased to 1 : 1, 2 : 3, 1 : 2, and 1 : 3, the coverage density of Fe_3O_4 nanoparticles on Ag NWs was markedly increased and the average particle sizes was about 8 nm. It is worth noting that the distribution of the particles along the surface of Ag NWs was homogeneous in both cases. Our method is thus able to fabricate Fe_3O_4 nanoparticles decorated Ag NWs with tunable size and coverage density, which offers an efficient way for fine tuning the magnetic properties of the final nanocomposites. The loading density of nanoparticles on Ag nanowires is increased as the raise of weight ratio of iron precursor. In the case of Ag/$Fe(acac)_3$ =1:2, 1:3, the Ag nanowires are almost fully covered by the Fe_3O_4 nanoparticles in a cluster state, which is shown in the TEM image of Fig. 4(i, j and k, l). The composition of the core shell heteronanowires(Fig. 4(i,j) was further confirmed by the energy-dispersive X-ray(EDX) spectrum(Fig. S3). The EDX results also demonstrate that the as-prepared product is mainly composed of Ag, Fe, C, O. These nanoparticles are firmly attached onto Ag NWs, indicating an excellent adhesion between Fe_3O_4 particles and Ag NWs is formed. It must be mentioned that when the mass ratio of Ag/$Fe(acac)_3$ is above 1:2, the excessive Fe_3O_4 nanoparticles which is not sticked to the Ag NWs were also observed.

In order to get a further understanding of the mechanism of selective deposition of Fe_3O_4 nanoparticles on Ag NWs, the formation process was investigated by TEM at different ratio between Ag NWs and $Fe(acac)_3$. A possible mechanism is proposed as follows. First, Fe ions decomposed by $Fe(acac)_3$ was bound on the the surface of Ag NWs by coordination of PVP, followed by partly reduced by TREG into very fine magnetite subparticles at elevated temperature. These subparticles have much high surface energy and are preferentially adsorbed on the surface of Ag NWs in polyol solution, serving as the nuclei of the ''secondary particles''. Nucleated Fe_3O_4 may, in turn, serve as seeds for further growth of Fe_3O_4 domains (Fig. S2). Later, multiple small Fe_3O_4 grains was formed on the surface of Ag NWs, rather than forming a continuous Fe_3O_4 shell. The neighboring subparticles were gathered by nuclei via van der Waals forces in addition to magnetic dipolar interactions.[31] Hererin in this work, PVP play vital role in forming the Ag NWs/Fe_3O_4 NPs composites, which is also confirmed by other previous works[21, 22, 32, 33]. This close interconnection between Ag cores and Fe_3O_4 shells is attributed to the PVP coated on Ag NWs. Additionally, it is amazing that the Fe_3O_4 NPs loaded on the Ag NWs exhibit prominent stability, which is also in accordance with other previous work.[34] After performing strong ultrasonication treatment for long time(excessive 30 miuntes), the Fe_3O_4 NPs loaded on the surface of NBs will not dislocate or fall off although some of the Ag NWs become shattered due to strong ultrasonic energy. The strong interaction may be attributed to PVP on the surface of Ag NWs since PVP could link Fe_3O_4 NPs readily and tightly.

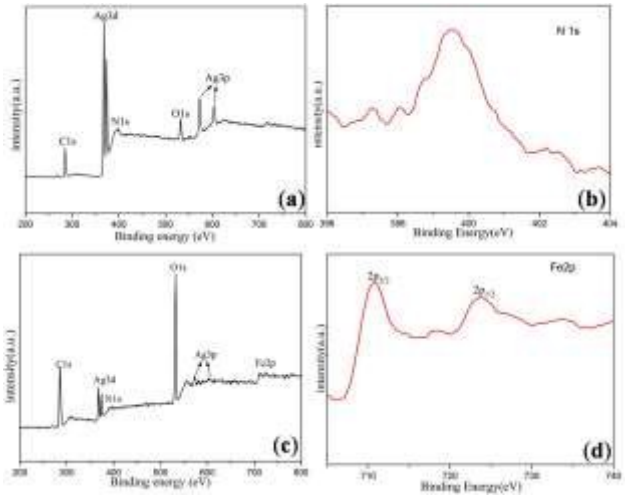

Fig. 5 XPS spectra wide scan of the AgNWs (a) , N1s spectra of the AgNWs(b) , wide scan of the Ag NWs/Fe_3O_4 NPs composites (c), and Fe2p spectra of the Ag NWs/Fe_3O_4 NPs composites (d).

To clarify the elemental and chemical states of Ag NWs/Fe_3O_4 NPs composites, XPS measurement is conducted on Ag NWs/Fe_3O_4 NPs composites prepared with an Ag content of 1.68 atom%. The corresponding results for Ag NWs with and without decorated Fe_3O_4 are shown in Fig. 5. All peaks on XPS curve for the composites are ascribed to Ag, Fe, O, N, and C. No any other peaks can be observed. This result confirms that Ag NWs/Fe_3O_4 NPs composites are composed of three elements of Fe, Ag, and O, which is consistent with the XRD and EDS results discussed above. As for as-prepared Ag NWs/Fe_3O_4 NPs composites, the Ag peak can still be found, even though the peak intensity was greatly lessened(Fig. S4). Comparison for XPS results of Ag NWs again verifies firmly that Ag nanowires have been fully covered by Fe_3O_4 nanoparticles. From Fig. S4 it can be seen that two peaks centered at 367.85 and 373.85 eV can be attributed to Ag 3d5/2 and Ag 3d3/2, respectively. In comparison with that of Ag NWs, the peak positions were almost kept the same as those of non-decorated. Peak positions of Ag 3d shift remarkably to lower binding energies compared with those of bulk Ag (Ag3d5/2, 368.2 eV; Ag 3d3/2, 374.2 eV), this phenomenon is similar to the results obtained from Ag-ZnO heterostructural nanofibers.[23] Then, the binding energy shift of Ag is mainly attributed to the coordination between the PVP and the surface of silver nanowires. Morover, the N1s (Fig. 5b) of Ag NWs exhibits one peak at 399.7 eV corresponding to the peak of PVP. This result fully proved that there exist PVP in the Ag NWs interface, which plays an important role as linker for hybrid formation. Therefore, the shift to lower binding energies of Ag 3d5/2 and Ag 3d3/2 further verifies the PVP role in the formation of Ag NWs/Fe_3O_4

NPs composites. It is worth mentioning the peak intensity of O1s of Ag NWs/Fe_3O_4 NPs composites was greatly improved, revealing that the TREG molecules was covered with Fe_3O_4 and then decorated onto the surface of Ag NWs. Thus, the surface hydroxyl is very important for dispersing in aquesous solution and functionability. Theses data, together with EDX, support the notion that the core shell nanowires are composed of silver nanowires and Fe_3O_4.

The magnetic properties of the as-made Ag NWs/Fe_3O_4 NPs composites were observed by a vibrating specimen magnetometer. Fig. 6 shows the representative hysteresis loops at room temperature of Ag NWs/Fe_3O_4 NPs composites with various MRs of Ag NWs to $Fe(acac)_3$. The curves show that the saturation magnetization (Ms) increases as the MR increases from 2 : 1 to 1 : 3, their saturation magnetizations are 18.6 (Fig. 6a), 10 (Fig. 6b) and 1.8 (Fig. 6c) emu.g^{-1}, respectively. The curves indicates that the magnetic properties significantly depend on the amount of Fe_3O_4 NPs decorated on the AgNWs. According to the curves we can find that the three samples exhibite superparamagnetic behavior at room temperature with no coercivity and remanence. Therefore, it is fully indicates that the magnetic properties of the nanocomposites can be easily adjusted by changing the mass ratio of precursor. These Ag NWs/Fe_3O_4 NPs composites could be quickly detached from their dispersion by holding the sample close to a commercial magnet. The magnetic properties of the decorated Ag NWs allow them to be easily manipulated by an external magnetic field, which is important to the applications.

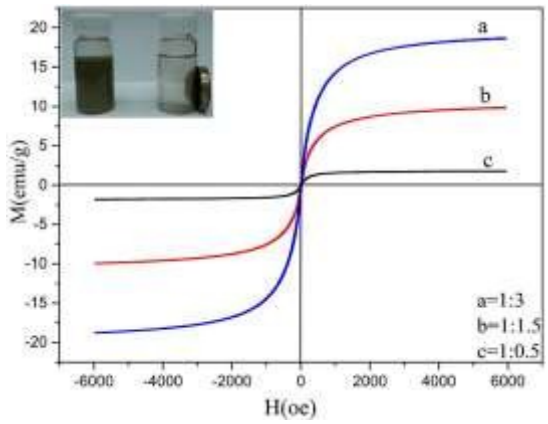

Fig. 6 Magnetic hysteresis curves measured at RT of Ag NWs/Fe_3O_4 NPs composites with various mass ratio of Ag NWs to $Fe(acac)_3$.

Despite of the good dispersion in aqueous solution, the Ag NWs/Fe_3O_4 NPs composites was also found to be dispersed in organic soultion such as EtOH, THF, Acetonitrile, and DMF(Fig. S5). These results fully indicate that these Ag NWs/Fe_3O_4 NPs composites are well dispersed into various solution due to the TREG well modified with Fe_3O_4.

The catalytic performance of Ag NWs/Fe_3O_4 NPs composites was explored in the reduction of MB dye, which was conducted in the presence of $NaBH_4$ as a model system.[35,36] Fig. 7 shows the UV–vis spectra for the reduction of MB measured at a different times during the progress of the reaction. It was found that the concentration of the MB decreased a little when the Ag NWs/Fe_3O_4 NPs composites was incubated with stock solution for 30 min, which may be respond to the absorbent property of the Ag NWs/Fe_3O_4 NPs composites (data not shown). After the addition of $NaBH_4$, the peaks at 610 and 665 nm gradually decreases in time, indicating the reducing of the MB dyes. The catalytic reduction of the dyes proceeds successfully, wherein no deactivation or poisoning of the catalyst is observed. No reaction can be observed without using the $NaBH_4$ or Ag NWs/Fe_3O_4 NPs composites. After the six recyclable experiment, many Fe_3O_4 nanopariticles were detached on the surface of the Ag NWs (Fig. S6), but the reduction efficiency was still kept as the same as the first time, indicating the well reduction eifficieny between the silver nanowire and MB dye. It must be mentioned the Ag NWs/Fe_3O_4 NPs composites can still be easily separated from the solution with the external magnetic field after the six recycle experiments, which renders the catalyst costeffective and promising for various applications.

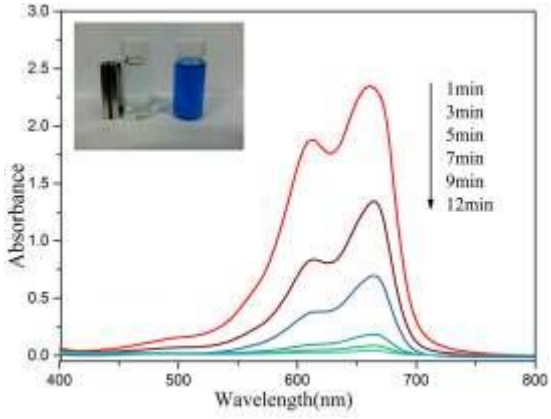

Fig. 7 UV-Vis absorption spectra of MB during the reduction catalyzed by Ag NWs/Fe_3O_4 NPs composites

Moreover, in order to further widen the application of the resultant composites, coated Fe_3O_4-decorated Ag NWs by organic(polymer) or inorganic(SiO_2) shells have also been explored for increasing the structural complexity and functionality of Ag NWs/Fe_3O_4 NPs composites. The Ag NWs/Fe_3O_4 NPs composites developed here is a versatile matrix for functionalization by coating Ag NWs/Fe_3O_4 NPs composites of various polymer, including SiO_2,[37] Polydopamine(Pdop),[38] PZS[39] and PFR.[40,41] Fig. 8 demonstrates that PFR, Pdop, PZS, SiO_2 coating can be easily achieved on the Ag NWs/Fe_3O_4 regardless of their reactive solvent system, as long as the surface properties can be mediated by using proper surfactants or not. Similar to the the Ag NWs/Fe_3O_4 composites, magnetic silver nanowires wrapped with the SiO_2, Pdop, PZS, PFR exhibit a rough surface, which can be attributed to the interfacial interaction between magnetic silver nanowire and polymer. This might well help to know the formation process of nanocables. The as-prepared polymer composites are believed to be able to find wide applications in e.g., biomaterials, drug delivery, supercapacitors etc.

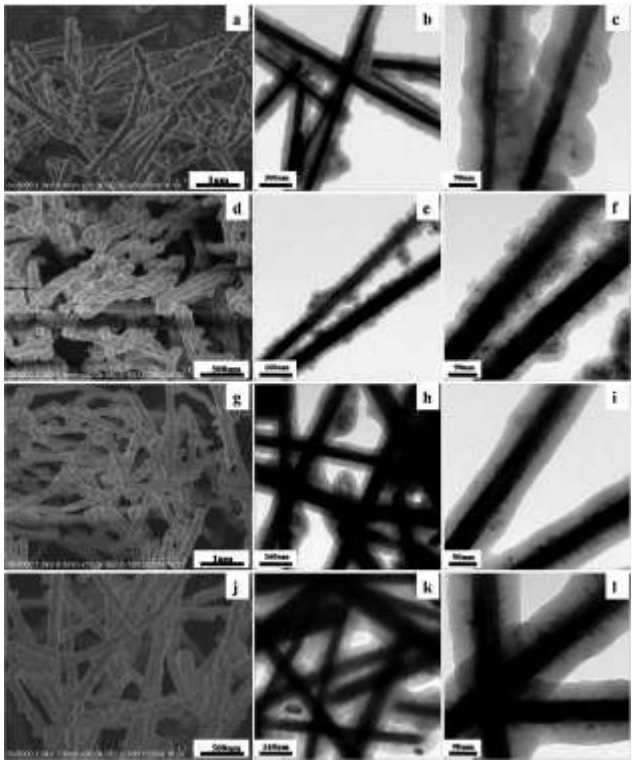

Fig. 8 The SEM and TEM images of the Ag NWs/Fe_3O_4 NPs composites@Polymer with different kinds of shells: (a,b,c)SiO_2, (d,e,f) Pdop, (g,h,i) PZS, (j,k,l)PFR.

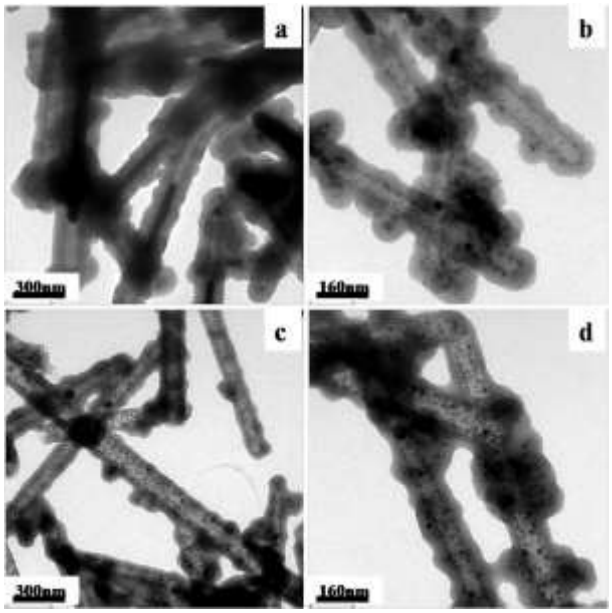

Fig. 9 The TEM images of the hollow magnetic silica nanotube with different time of etching Ag NWs in ammonia and H_2O_2 : (a,b)One day, (c,d) three days.

As pointed out in the previous work,[42] Ag nanowires can serve as physical templates, leading to the formation of 1D hollow nanostructures. Hererin in this work, Ag NWs/Fe_3O_4@SiO_2 was selected as a model to test its feasiblity.

To produce hollow magnteic silica nanotube, a mixture of aqueous ammonia (5 mL, 27 wt %) and H_2O_2 (5 mL, 30 wt %) with a pH value of 9.0 was used to eliminate the silver cores within the Ag NWs/Fe_3O_4@SiO_2. As FESEM image (Fig. S7) demonstrated that the majority of the samples are composed of sub-microfibers. A typical TEM image showed that the silver core can be partly removed from its interior if the sub-microcables are kept in the solution for one day (Fig.9(a,b)). Contiue etching the silver nanowires as long as three days, the magnetic hollow silica nanotube can be obtained(Fig.9(c,d)). It must be mentioned that the trace content of silver is still observed, which is also in accordance with the data of XRD(Fig. S8). Compared to Yu's work, the speed of etching is lower, which is due to the the different properties between cross-linked PVA and silica. The cross-linked PVA polymer is more easier to permeate the small molecules such as ammonia and H_2O_2, this will contribute to dissolve the template of Ag NWs to obtain the hollow structures with higher speed. As such, the other magnetic hollow nanotubes could be obtained using others Ag NWs/Fe_3O_4@Polymer, further work is underway.

Conclusions

In summary, we have demonstrated a facile and efficient solution-phase method to in situ synthesis Ag NWs/Fe_3O_4 NPs composites by high-temperature decomposition of the precursor iron(III) acetylacetonate and Ag NWs in liquid polyols. The method is simple and highly efficient, and Ag NWs can be used directly without any other pretreatment procedures. Moreover, the loading density of magnetite nanoparticles on the surface of Ag NWs can be tunable in this method, which offers an efficient way for tuning the magnetic properties of the final nanocomposites. The resulting hybrid nanomaterials can be easily dispersed in aqueous and organic solution and have applications in catalyzing the MB dye for wastewater treatment. More importantly, the resultant composites can be well coated by silica, Pdop, PFR, PZS, which will greatly widen the applications of the Fe_3O_4 -decorated Ag NWs. The last but not the least, the Ag NWs core can be physical template to obtain the magnetic hollow nanotube materials. We believe that the synthetic hybrid composites described in this paper can be extended to deposition of other metals, alloys, or oxides nanoparticles onto Ag NWs surface by selecting appropriate precursors and polyol solvents.

Acknowledgements

The authors are grateful to the financial support by the National Science Foundation of China (No 21305086). The Natural Science Foundation of Shanghai City (13ZR141830), Research Innovation Program of Shanghai Municipal Education Commission (14YZ138), the Special Scientific Foundation for Outstanding Young Teachers in Shanghai Higher Education Institutions (ZZGJD13016), Start-up Funding of Shanghai

University of Engineering Science, Shanghai Municipal EducationCommission (Overseas Visiting Scholar Project 20120407), Shanghai Young Teachers' Training-funded Projects(ZZGJD13018), Shanghai University of Engineering ScienceDeveloping founding (grant 2011XZ04), start-up project funding (grant 0501-13-018) and Interdisciplinary Subject Construction (grant 2012SCX005).

Note and References

College of Chemistry and Chemical Engineering, Shanghai University of Engineering Science, Shanghai 201620, China. E-mail: zhangmin@sues.edu.cn; polymer07@sina.com; xujingli@sues.edu.cn;

References

1 S.J.Guo , E.K.Wang , *Acc. Chem. Res.*, 2011, **44**, 491.

2 J.Coraux, L.T.Marty , N.Bendiab, et al. *Acc Chem Res.*, 2012,**46**, 2193.

3 X.Huang ,X.Y.Qi , F.Boey and H.Zhang, *Chem. Soc. Rev.*, 2012, **41**, 666.

4 M.B.Cortie and A.M.McDonagh, *Chem. Rev.*,2011, **111**, 3713.

5 D. Eder ,*Chem. Rev.*, 2010, **110**, 1348 .

6 J. F. Shi, Y. J. Jiang, X. Wang, H. Wu, D. Yang, F.S.Pan, Y.L.Suad and Z.Y.Jiang, *Chem. Soc. Rev.*, 2014, **43**, 5192.

7 H.W.Liang , J. W. Liu , H. S. Qian , and S. H. Yu , *Acc. Chem. Res.*, 2013, **46**,1450.

8 M. R. Gao, Y. F. Xu, J. Jiang and S.H.Yu, *Chem. Soc. Rev.*, 2013, **42**, 2986.

9 C.Sanchez, P.Belleville, M.Popalld and L.Nicole, *Chem. Soc. Rev.*, 2011, **40**, 696.

10 J. Ge, H. B. Yao, X. Wang, Y. D. Ye, J. L. Wang, S. H. Yu , *Angew. Chem. Int. Ed.*, 2013, **52**, 1655.

11 H. R Liu, G.X.Shao, J.F.Zhao, *J.Phys.Chem.C.*, 2012,**116**,16182.

12 N.C.Bigall,W.J.Paraka,D.Dorfs,*Nano.Today* ., 2012, **7**, 282.

13 S.W.Wang,Y.Yu,Y.H.Zuo, C.Z.Li, J. H. Yang and C. H. Lu ,*Nanoscale*, 2012, **4**, 5895.

14 H. Eom , J. Lee , A. Pichitpajongkit , M. Amjadi , J.H. Jeong , E. Lee , J. Y. Lee , and I.Park,*Small*,2014,**10**,4171.

15 J.Y.Xiong,Z. Li, J.Chen, S.Q.Zhang, L.Z. Wang and S.X.Dou,*ACS. Appl. Mater. Interfaces.*, 2014, **6**, 15716.

16 B.Cheng, Y. Le, J.G.Yu, *J.Hazardous.Materials*, 2010, **177**, 971.

17 P.Ramasamy, D.Min.Seo, S.H.Kima and J.K.Kim, *J. Mater. Chem.*, 2012,**22**,11651

18 Y.Sun, Z.Tao, J.Chen, T.Herricks, Y.Xia,*J. Am. Chem. Soc.*, 2004, **126**, 5940.

19 Y.P.Bi, J.H.Ye, *Chem .Commun.*, 2009,**43**, 6551.

20 Y.G.Sun, *J. Phys. Chem. C.*, 2010, **114** , 2127.

21 H.Hu, Z.Jiao,T.Y.Wang, G.Lu,Y.Bi, *J.Mater. Chem. A.*, 2013, **1**, 10612.

22 Y.Bi, H.Hu, S.O.Yang, Z.Jiao,G.Lu, J.Ye, *J. Mater. Chem.*, 2012, **22**, 14847.

23 N.Li, G.W.Huang, X.J.Shen, H.M.Xiao and S. Yun, *J. Mater. Chem. C.*, 2013, **1**, 4879.

24 Y.M. Zhai, L.Han, P.Wang, G.P.Li, W. Ren, L.Liu, E.Wang, and S.J.Dong ,2011, *ACS .Nano.*, **11**, 8562.

25 J.Ge,H.B.Yao,X.Wang,*Angew.Chem.Int.Ed.*, 2013, **125**, 1698.

26 J. Q.Wan, W. Cai, J. T. Feng, X. X. Meng and E. Z. Liu, *J. Mater. Chem.*, 2007, **17**, 1188.

27 C.Yang, H.W.Gu,W.Lin ,M. Matthew , C. P .Wong , M.Y.Xiong , and B.Gao, *Adv. Mater.*,2011, **23**, 3055.

28 X. Z. Wang, Z. B. Zhao, J. Y. Qu, Z. Y. Wang and J. S. Qiu,*J. Phys. Chem. Solids.*, 2010, **71**, 673.

29 J. H .Sui , J. Li , S. J.Yang , Z. G. Li , W. Cai, *Mater. Lett* .,2013, **100**, 33.

30 T.Rajh, L.X.Chen, K.Lukas, T.Liu, M.C. Thurnauer, D.M. Tiede,*J. Phys. Chem.B*, 2002,**106**,10543.

31 J. Wan and W. Cai, *J.Colloid Interface.Sci.*, 2007, **305**, 366.

32 Y. Y. Liu, W. N. Zhang, S. Z. Li, C. L. Cui, J. Wu, H. Y. Chen, F. W. Huo. *Chem. Mater.*, 2014, **26**, 1119.

33 H. Sun, J. T. He, J. Y. Wang, S. Y. Zhang, C. C. Liu, T. M. Sritharan, S. Mhaisalkar, M. Y. Han, Dan, Wang, H. Y. Chen. *J. Am. Chem. Soc.*, 2013, **135**, 9099.

34 M. R .Gao, S. Liu, J. Jiang, C. H. Cui, W. T. Yao and S.H. Yu, *J. Mater. Chem.*, 2010,**20**, 9355.

35 M. Zhang, P. Xia, L. Wang, J. Zheng, Y. Wang, J. Xu and L. Wang, *RSC Adv.*, 2014, **4**, 44423.

36 M. Zhang, J. Zheng, P. Xia, Y. Zheng, J. Xu, L. Chen, X. He and Q. Fang, *New J. Chem.*, 2014, **38**, 3212.

37 Y.H. Deng, D.W. Qi, C.H Deng, X.M. Zhang, and D.Y.Zhao, *J. Am. Chem. Soc.*, 2008, **130**, 28

38 M. Zhang, J. Zheng, Y. Zheng, J. L.Xu, X. W. He, L. X. Chen and Q.L.Fang, *RSC.Adv.*, 2013, **3**, 13818.

39 J.W. Fu, X.B.Huang, Y.W. Huang, Y.Pan, Y.Zhu, and X.Z. Tang, *J. Phys. Chem. C.* , 2008, **112**, 16840.

40 X.L.Fang, S.J.Liu, J.Zang, C.F. Xu, M.S.Zheng,Q.F. Dong, D.H. Sun and N.F. Zheng, *Nanoscale*, 2013, **5**, 6908.

41 N. Li, Q. Zhang, J. Liu, J.B. Joo, A .Lee, Y. Gan and Y.D.Yin, *Chem. Commun.*, 2013, **49**, 5135.

42 L. B. Luo, S. H. Yu, H. S. Qian, Gong, J. Y. Gong, *Chem-Eur J*, 2006, **12**, 3320.